DESIGN OF AN END EFFECTOR FOR CRAWLING ROUNDLIKE FRUITS

Yinggang Shi, Yang Guo, Li Liu, Jizheng Zhao, Jun Chen, Yongjie Cui

ABSTRACT: In order to improve the adaptability of the end effectors when crawling roundlike fruits such as apples, pears and peachs in complex environment, a new design of the mechanical structure of the end effectors was proposed through analyzing the characteristics of roundlike fruits, the end effectors having the quasi hand five-finger structure was adopted to replace simple two-finger and three-finger structures. At the same time, the mechanical strength of the finger was checked. Then with the help of robot kinematics, the poses, speed and acceleration of the fingertip were analyzed. The finger movements were planned through using the S curve speed planning method. And the action and force situation of the end effectors were simulated to check the performances of the motor.
KEY WORDS: roundlike, the end effector, kinematics, trajectory planning.

1 INTRODUCTION

Agricultural products are usually delicate and difficult to handle [1]. Therefore, a high requirement is placed on the mechanical control and feedback of the end effectors. Among relevant studies [2-13], the picking of a single type of fruit is usually concerned, which lacks universality. Many studies only consider the automatic gripping and picking of a single fruit, while in practice, the end effector can hardly work under the ideal environment due to the limitations of agricultural field, sheltering by the fruits and dense growth of the fruits. Moreover, the fruits may have varying shapes during the picking, grading and packaging operations. The proper working of three- or four-finger end effectors usually requires specific shape and position of the fruits and a high gripping force. To achieve this, the end effectors should have high sensor precision and optimized control algorithm. But few studies are devoted to the design of end effector specialized for intermediates operations such as fruit thinning and bagging.

Addressing the above problems, the paper designed an end effector by mimicking human hand's to crawl roundlike fruits and vegetables, which increases the contact area and friction with the fruits and makes the gripping force more uniform [14]. This gripper can adapt to various environments and achieve flexible gripping and picking of fruits at reduced mechanical injury to the fruits. After design optimization, this end effector can be applied to fruit grading, sorting and bagging with higher agricultural automation and lower cost.

College of Mechanical and Electronic Engineering, Northwest A&F University, NO.3 Taicheng Road, Yangling 712100, Shaanxi, P.R.China

E-mail: liuli_ren_79@nwsuaf.edu.cn

2 MECHANICAL DESIGN OF THE END EFFECTOR

The roundlike fruits such as apples, pears, peaches, kiwi fruits, tomatoes and round eggplant are considered as round. The diameter of a tomato is generally 50mm-70mm and the mass is 70-140kg; the diameter of an apple is 60mm-100mm with mass of about 0.25kg[15]. Apples, pears and kiwi fruits have larger size and density among the above roundlike fruits. The end effector is designed based on the size and requirement for picking apples as well as the planting area.

For the picking of supreme premium apples, the total area of compression should not exceed 1cm2[16]. Thus the end effector that mimicks the human hand is designed based on this requirement [17]. In the new structure of robot gripper, the thumb is located in the palm to assist the picking operation of the other four fingers, as shown in Fig. 1.

The four fingers, forefinger, middle finger, third finger and fourth finger, share the same structure, each having 4 degrees of freedom. The 4 degrees of freedom refer to the tilting of distal interphalangeal joint, middle joint and basal joint and the lateral swinging of the basal joint. The spacing between two adjacent fingers is 18mm. The length and width of the distal interphalangeal joint are 20mm and 18mm, respectively; the length and width of the middle joint are 30mm and 24mm, respectively; the length and width of the basal joint are 40mm and 18mm, respectively. Since the thumb does not swing laterally, the thumb has 3 degrees of freedom in tilting. The length and width of the joint of thumb are the same as those of the other four fingers.

The structures of forefinger, middle finger, third finger and fourth finger are shown in Fig. 2. Motor 1 and motor 2 drive the transmission belt, delivering force to axle 1 and axle 2 of the differential mechanism of the basal joint, as shown in Fig. 3. The axles of motor 1 and motor 2 will turn towards human, and the clockwise rotation of the axles corresponds to the forward rotation of the motor. Then, when motor 1 and motor 2 in Fig. 2 rotate in a forward or reverse direction simultaneously, axle 1 and axle 2 in Fig. 3 also rotate in a forward or reverse direction simultaneously. They drive the rotation of the driving bevel gear 1 and driving bevel gear 2 in the reverse or forward direction simultaneously. Under the action of moment of force with equal magnitude and opposite direction, the driven bevel gear 3 and driven bevel gear 4 maintain a dynamic balance without rotation. The rotation of driving bevel gear 1 and driving bevel gear 2 will drive the tilting of the entire fingers. When motor 1 and motor 2 in Fig. 2 rotate in different directions, the driving bevel gear 1 and driving bevel gear 2 will rotate in the corresponding directions under the action of axle 1 and axle 2 in Fig. 3. The driven bevel gear 3 and driven bevel gear 4 are made to rotate in the reverse and forward direction around axle 3 and axle 4 under the action of two times of torsional moment in the reverse and forward direction, respectively. As a result, the fingers swing laterally. In Fig. 2, motor 3 and motor 4 drive the rotation of the middle joint and distal interphalangeal joint, respectively.

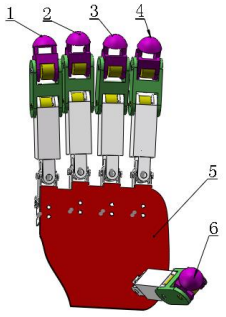

Figure 1. Mechanical design of end effector
1. Fourth finger; 2. Third finger; 3. Middle finger; 4. Forefinger; 5. Palm; 6. Thumb

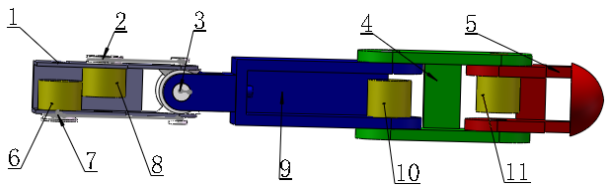

Figure 2. Structure of forefinger, middle finger, third finger and fourth finger

1. Groove for installing the fingers; 2. Transmission belt; 3. Differential mechanism of basal joint; 4. Middle joint; 5. Distal interphalangeal joint; 6. Motor 1; 7. Transmission belt; 8. Motor 2; 9. Proximal interphalangeal joint; 10. Motor 3; 11. Motor 4

For the basal joints of each finger, a total of 16 pairs of curved tooth bevel gears with the same structure are designed. The design parameters are shown in Table 1. The middle joints and distal interphalangeal joints of forefinger, middle finger, third finger and fourth finger are directly driven by the motors; the basal joints are driven by the transmission belt powered by the motor. The TRUM-30 type ultrasonic motor developed by Precision Driving Institute of Nanjing University of Aeronautics and Astronautics is used. The diameter of the stator is 30mm and the rated torsional moment is 50N·mm; the maximum output torsional moment is 200N·mm, the maximum rotational speed 250r/min, and dead weight 40g[18].

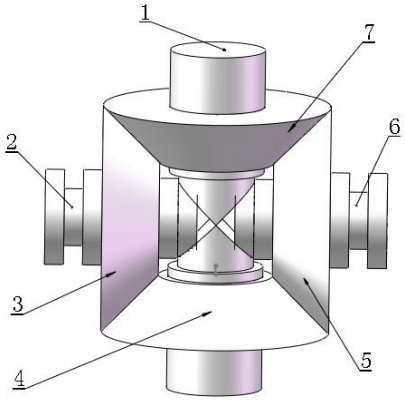

1.Axle 3; 2. Axle 1; 3. Driving bevel gear 1; 4. Driven bevel gear 4; 5. Driving bevel gear 2; 6. Axle 2; 7. Driven bevel gear 3

(a) Basal joint

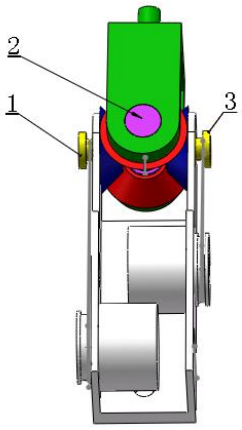

(b) Transmission mechanism of basal joint

Figure 3. Force transmission to the differential mechanism of basal joint

The thumb has 3 degrees of freedom correspond the rotation of the 3 joints. The motor driving the gear and the basal joint is located beneath the palm, as shown in Fig. 4.

Table 1. Parameters of curved tooth bevel gear

Modulus m	0.5mm
Tooth number z	20
Pressure angle α	20°
Width of gear b	3mm
Addendum coefficient ha*	1
Tooth clearance coefficient c*	0.02
Modification coefficient	0
Helical angleβ	35°

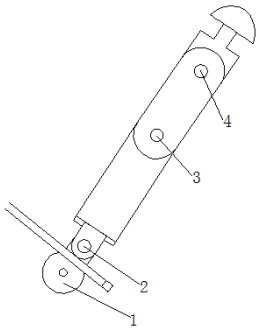

1. Motor of basal joints and big gear; 2. Small gear; 3. Motor 2; 4. Motor 3

Figure 4. Sectional view of thumb

In extreme conditions, the finger tips bear all the weight of the fruits. Consider an apple with maximum mass of about 0.25kg. When distributed to each finger, the load is about 0.7N. The middle finger bears the largest load during picking. For simulation of the mechanical strength of the finger, the load of 1N is imposed on the tip of the middle finger with its basal joint fixed. The end effector is made of 1060 aluminum alloy, with shear modulus of 2.7*1010N/m2, density of 2700Kg/m3, yield strength of 27574200N/m2, elastic modulus of 6.9*1010N/m2 and Poisson's ratio of 0.33. The loading pattern, stress, displacement, strain and stress of the middle finger are shown in Fig. 5a, b, c and d, respectively. The simulation indicates that the minimum shear stress is 63.8523N/m2 and the maximum is 375964N/m2; the minimum displacement is 0mm and the maximum is 1.09785×10-3mm; the minimum strain is 1.40987×10-9 and the maximum is 3.75547×10-6. The mechanical strength of the middle finger satisfies the requirement, and so does the mechanical strength of other fingers.

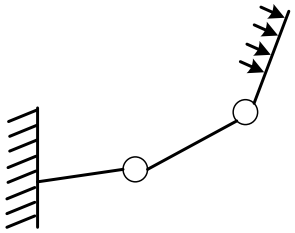

a) Loading pattern of middle finger

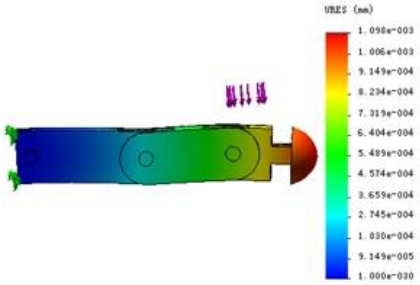

b) Displacement of middle finger

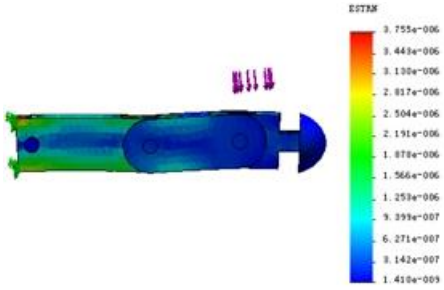

c) Strain of middle finger

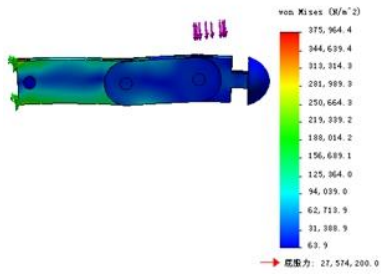

d) Stress of middle finger

Figure. 5 Simulation of mechanical strength of middle finger

3 REQUIREMENTS FOR THE PAPER

Kinematic analysis of the end effector is performed with respect to the posture, speed and acceleration of finger tips.

To stably grip the fruits, the end effector must have accurate gripping posture based on the contour of the fruits. Through inverse kinematic analysis of the robot, the rotation angle of each joint can be obtained for a given posture. Through forward

kinematic analysis, the rotation angle of each joint and the relationship with the posture of the finger tips are obtained. Thus, the desired rotation angle of the joint is achieved by the control algorithm. By analyzing the robot Jacobian, the gripping force exerted by the finger tip is calculated. The kinematic parameters of the finger point are then converted into the kinematic parameters of each joint. The motion of each joint is constantly adjusted during picking so as to reduce the damage of the gripper to the fruits.

3.1 Forward kinematic analysis

Using D-H method[19], the kinematic coordinates of the middle finger are established, as shown in Fig. 6. The D-H parameters of the middle finger are given in Table 2.

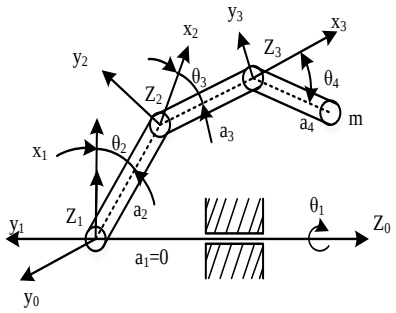

Figure. 6 Structural parameters and coordinates of the middle finger

Table 2 D-H parameter of the middle finger

Connecting rod	$\theta_i a_i$	$a_i a_i$(mm)	d_i	α_i(°)	Range
1	θ_1	0	0	90	-5～5
2	θ_2	40	0	0	-90～90
3	θ_3	30	0	0	-90～90
4	θ_4	20	0	0	-90～90

Suppose $s_i = \sin(\theta_i), c_i = \cos(\theta_i),\ s_{ijk} = (\theta_i + \theta_j + \theta_k),\ c_{ijk} = (\theta_i + \theta_j + \theta_k)$, then the rotation matrices A_1, A_2, A_3 and A_4 are are

$$A_1 = \begin{bmatrix} c_1 & 0 & s_1 & 0 \\ s_1 & 0 & -c_1 & 0 \\ 0 & 1 & 0 & 0 \\ 0 & 0 & 0 & 1 \end{bmatrix},\quad A_2 = \begin{bmatrix} c_2 & -s_2 & 0 & a_2 c_2 \\ s_2 & c_2 & 0 & a_2 s_2 \\ 0 & 1 & 1 & 0 \\ 0 & 0 & 0 & 1 \end{bmatrix},$$

$$A_3 = \begin{bmatrix} c_3 & -s_3 & 0 & a_3 c_3 \\ s_1 & c_3 & 0 & a_3 s_3 \\ 0 & 0 & 1 & 0 \\ 0 & 0 & 0 & 1 \end{bmatrix},\quad A_4 = \begin{bmatrix} c_4 & -s_4 & 0 & a_4 c_4 \\ s_4 & c_4 & 0 & a_4 s_4 \\ 0 & 0 & 1 & 0 \\ 0 & 0 & 0 & 1 \end{bmatrix}$$

Let ${}^0T_4$ be the homogeneous coordinate transformation matrix of the finger tip with respect to coordinate 0, then

$${}^0T_4 = A_1 * A_2 * A_3 * A_4 = \begin{bmatrix} c_1 c_{123} & -c_1 s_{234} & s_1 & (a_3 c_{23} + a_4 c_{234} + a_2 c_2) c_1 \\ s_1 c_{234} & -s_1 s_{234} & -c_1 & (a_3 c_{23} + a_4 c_{234} + a_2 c_2) s_1 \\ -s_{234} & -c_{234} & 0 & a_3 s_{23} + a_4 s_{234} + a_2 s_2 \\ 0 & 0 & 0 & 1 \end{bmatrix} \quad (1)$$

The transformation matrix of the finger tip with respect to the reference coordinate system is expressed as follows:

$${}^0T_4 = \begin{bmatrix} n_x & o_x & a_x & p_x \\ n_y & o_y & a_y & p_y \\ n_z & o_z & a_z & p_z \\ 0 & 0 & 0 & 1 \end{bmatrix} \quad (2)$$

The values of $\theta_1 \theta_2 \theta_3 \theta_4$ are given, and by substituting the length of each joint, the position and posture of the tip of the middle finger are calculated according to formula (1) and (2), respectively.

The calculation is the same with forefinger, third finger and fourth finger and the details are not repeated here.

Since the thumb has only 3 degrees of freedom, let $A_1' = A_2$, $A_2' = A_3$ $A_3' = A_4$. Thus, the transformation matrix of the tip of the thumb with respect to the reference coordinate system is as follows:

$${}^{0\prime}T_3 = A_1' * A_2' * A_3' = \begin{bmatrix} n_x & o_x & a_x & p_x \\ n_y & o_y & a_y & p_y \\ n_z & o_z & a_z & p_z \\ 0 & 0 & 0 & 1 \end{bmatrix} \quad (3)$$

3.2 Inverse kinematic analysis

Given the posture of the finger tips, the rotation angle of each joint can be known. From ${}^0T_4 = A_1 * A_2 * A_3 * A_4$, it is obtained that

$$p_x = a_1 \cos\theta_1 + a_2 \cos\theta_1 \cos\theta_2 + a_3 \cos\theta_1 \cos\theta_2 \cos\theta_3 - a_3 \cos\theta_1 \sin\theta_2 \sin\theta_3 \quad (4)$$

$$p_y = a_1 \sin\theta_1 + a_2 \cos\theta_2 \sin\theta_1 + a_3 \cos\theta_2 \cos\theta_3 \sin\theta_1 - a_3 \sin\theta_1 \sin\theta_2 \sin\theta_3 \quad (5)$$

$$p_z = a_2 \sin\theta_2 + a_3 \cos\theta_2 \sin\theta_3 + a_3 \cos\theta_3 \sin\theta_2 \quad (6)$$

Hence

$$\theta_1 = \arctan\frac{p_y}{p_x}$$

Let $\theta_4 = k * \theta_3$, then $\theta_3 + \theta_4 = (k+1)\theta_3$, i.e.,

$$a_4 c_{234} + a_3 c_{23} + a_2 c_2 = \frac{p_x}{c_1} = \frac{p_y}{s_1}$$

Let $p_{xy} = \frac{p_x}{c_1} = \frac{p_y}{s_1}$, and according to formula (4), (5) and (6)

$$\frac{1}{a_2}\cos(k\theta_3) + \frac{1}{a_3}\cos(k\theta_3 + \theta_3) + \frac{1}{a_4}\cos(\theta_3) = \frac{p_{xy}^2 + p_z^2 - a_2^2 - a_3^2 - a_4^2}{2a_2a_3a_4} \quad (7)$$

From formula (7), θ_3 and θ_4 are calculated.

From formula (4), (5) and (6), it is obtained that

$$(a_4 s_{34} + a_3 s_3)c_2 + (a_4 c_{34} + a_3 c_3 + a_2)s_3 = -p_z$$

Let

$C = a_4 s_{34} + a_3 s_3$ and

$D = a_4 c_{34+} a_3 c_{3+} a_2$, thus

$$\theta_2 = \tan^{-1}\frac{p_z}{\sqrt{C^2 + D^2 - p_z^2}} - \tan^{-1}\frac{C}{D}$$

θ_1, θ_2, θ_3 and θ_4 are the rotation angles of the joints of middle finger, forefinger, third finger and fourth finger, respectively, given the posture of the finger tips. The calculations of the rotation angles of the joints of forefinger, third finger and fourth finger are the same as that with the forefinger.

Similarly, the rotation anglesθ_1, θ_2 and θ_3 of the joints of the thumb are obtained.

$${}^1T_4 = A_2 * A_3 * A_4 = \begin{bmatrix} c_{234} & s_{234} & 0 & a_3c_{23} + a_4c_{234} + a_2c_2 \\ c_{234} & c_{234} & 0 & a_3s_{23} + a_4s_{234} + a_2s_2 \\ -s_{234} & 0 & 1 & 0 \\ 0 & 0 & 0 & 1 \end{bmatrix}$$

Let $\theta_2 = k * \theta_3$

$$p_x = a_3c_{23} + a_4c_{234} + a_2c_2 \quad (8)$$

$$p_y = a_3s_{23} + a_4s_{234} + a_2s_2 \quad (9)$$

From (8) and (9), it is known that

$$\left(\frac{px - a_3c_{23} - a_2c_2}{a_4}\right)^2 - \left(\frac{py - a_3s_{23} - a_2s_2}{a_4}\right)^2 = 1 \quad (10)$$

The values of θ_2 and θ_3 calculated by formula (10) are substituted into formula (8) to get θ_4. The values of θ_2, θ_3 and θ_4 correspond to θ_1, θ_2 and θ_3 in the coordinate system of the thumb, respectively.

The inverse kinematic equations of the fingers have several solutions, from which the appropriate one is chosen based on specific need and steadiness requirement of motion.

3.3 Jacobian analysis

The Jacobian of the forefinger, middle finger, third finger and fourth finger can be expressed as follows:

$$J_{(q)} = [J_1 \quad J_2 \quad J_3 \quad J_4]$$

where

$$J_i = \begin{bmatrix} Z_{i-1} \times {}^0P_n^{i-1} \\ Z_{i-1} \end{bmatrix} = \begin{bmatrix} Z_{i-1} \times ({}^0R_{i-1}{}^{i-1}P_n^{i-1}) \\ Z_{i-1} \end{bmatrix} \quad (11)$$

where ${}^0R_{i-1}$ is the transformation matrix of ${}^0R_{i-1}$ in coordinate system {i-1} with respect to the reference coordinate system {0}:

$${}^0R_0 = \begin{bmatrix} 1 & 0 & 0 \\ 0 & 1 & 0 \\ 0 & 0 & 1 \end{bmatrix}, \quad {}^0R_1 = \begin{bmatrix} c_1 & 0 & s_1 \\ s_1 & 0 & -c_1 \\ 0 & 1 & 0 \end{bmatrix},$$

$${}^0R_2 = \begin{bmatrix} c_1c_2 & -c_1s_2 & s_1 \\ s_1c_2 & -s_1s_2 & -c_1 \\ s_2 & c_2 & 0 \end{bmatrix},$$

$${}^0R_3 = \begin{bmatrix} c_1c_{23} & -c_1s_{23} & s_1 \\ s_1c_{23} & -s_1s_{23} & -c_1 \\ s_{23} & c_{23} & 0 \end{bmatrix}$$

${}^{i-1}P_n^{i-1}$ is the representation of the origin of coordinate system {n} in the reference coordinate system with respect to the coordinate system {i-1}:

${}^0P_n^{i-1} = {}^0R_{i-1} * {}^{i-1}P_n^{i-1}$

i.e.,

$${}^0P_4^0 = \begin{bmatrix} (a_4c_{234} + a_3c_{23} + a_2c_2)c_1 \\ (a_4c_{234} + a_3c_{23} + a_2c_2)s_1 \\ a_4s_{234} + a_3s_{23} + a_2s_2 \end{bmatrix},$$

$${}^1p_4^1 = \begin{bmatrix} a_4c_{234} + a_3c_{23} + a_2c_2 \\ a_4s_{234} + a_3s_{23} + a_2s_2 \\ 0 \end{bmatrix},$$

$${}^2p_4^2 = \begin{bmatrix} c_3a_4c_4 - s_3a_4s_4 + a_3c_3 \\ s_3a_4\ c_3 + c_3a_4 + a_3s_3 \\ 0 \end{bmatrix},$$

$${}^3p_4^3 = \begin{bmatrix} a_4c_4 \\ a_4s_4 \\ 0 \end{bmatrix}$$

Z_{i-1} is the unit vector of z axis in the coordinate system {i-1}.

$$Z_0 = \begin{bmatrix} 0 \\ 0 \\ 1 \end{bmatrix}, \quad Z_1 = \begin{bmatrix} s_1 \\ -c_1 \\ 0 \end{bmatrix}, \quad Z_2 = \begin{bmatrix} s_1 \\ -c_1 \\ 0 \end{bmatrix}, \quad Z_3 = \begin{bmatrix} s_1 \\ -c_1 \\ 0 \end{bmatrix}$$

Substituting ${}^0R_{i-1}$, P_n^{i-1} and Z_{i-1} into formula (11) will produce

$$J_1 = \begin{bmatrix} -(a_4c_{234} + a_3c_{23} + a_2c_2)s_1 \\ (a_4c_{234} + a_3c_{23} + a_2c_2)c_1 \\ 0 \\ 0 \\ 0 \\ 1 \end{bmatrix} \quad (12)$$

$$J_2 = \begin{bmatrix} -c_1(a_4c_{234} + a_3c_{23} + a_2s_2) \\ -s_1(a_4s_{234} + a_3s_{23} + a_2s_2) \\ a_4c_{234} + a_3c_{23} + a_2c_2 \\ s_1 \\ -c_1 \\ 1 \end{bmatrix}$$

(13)

$$J_3 = \begin{bmatrix} -c_1[s_2(c_3a_3c_4 - s_3a_4s_4 + a_3s_3) + c_2(s_3a_4c_4 + c_3a_4s_4 + a_3s_3) \\ -s_1[s_2(a_4 - s_3a_4s_4 + a_3s_3 + a_3s_3) + c_2(s_3a_4c_4 + c_3a_4s_4 + a_3s_3) \\ a_4c_{234} + a_3c_{23} + a_2c_2 \\ s_1 \\ -c_1 \\ 1 \end{bmatrix}$$

(14)

$$J_4 = \begin{bmatrix} -c_1(s_{23}a_4c_4 - c_{23}a_4s_4) \\ -s_1(s_{23}a_4c_4 - c_{23}a_4s_4) \\ s_{23}a_4c_4 - a_4s_4s_{23} \\ s_1 \\ -c_1 \\ 1 \end{bmatrix}$$

(15)

where $\dot{x}$ is the speed of finger tip; $\dot{q}$ is the speed of the joint, thus

$$\dot{x} = J_{(q)} * \dot{q}$$

$$\ddot{x} = J_{(q)} * \ddot{q} + \dot{J}_{(q)} * \dot{q}$$

From formula (12), (13), (14) and (15), the relations of joint speed and acceleration to finger tip speed and acceleration can be obtained, thus achieving the mapping of the joint space to the operating space.

Similarly, the transformation matrices of the thumb are calculated:

$${}^0R_0 = \begin{bmatrix} c_1 & 0 & s_1 \\ s_1 & 0 & -c_1 \\ 0 & 1 & 0 \end{bmatrix},$$

$${}^0R_1 = \begin{bmatrix} c_1c_2 & -c_1s_2 & s_1 \\ s_1c_2 & -s_1s_2 & -c_1 \\ s_2 & c_2 & 0 \end{bmatrix},$$

$${}^0R_2 = \begin{bmatrix} c_1c_{23} & -c_1s_{23} & s_1 \\ s_1c_{23} & -s_1s_{23} & -c_1 \\ s_{23} & c_{23} & 0 \end{bmatrix}$$

$$Z_0 = \begin{bmatrix} s_1 \\ -c_1 \\ 0 \end{bmatrix}, Z_1 = \begin{bmatrix} s_1 \\ -c_1 \\ 0 \end{bmatrix},$$

$$Z_2 = \begin{bmatrix} s_1 \\ -c_1 \\ 0 \end{bmatrix} A_1 = \begin{bmatrix} c_1 & -s_1 & 0 & a_2c_1 \\ s_1 & c_1 & 0 & a_2s_1 \\ 0 & 1 & 1 & 0 \\ 0 & 0 & 0 & 1 \end{bmatrix},$$

$$A_2 = \begin{bmatrix} c_2 & -s_2 & 0 & a_3c_2 \\ s_2 & c_2 & 0 & a_3s_2 \\ 0 & 0 & 1 & 0 \\ 0 & 0 & 0 & 1 \end{bmatrix},$$

$$A_3 = \begin{bmatrix} c_3 & -s_3 & 0 & a_4c_3 \\ s_3 & c_3 & 0 & a_4s_3 \\ 0 & 0 & 1 & 0 \\ 0 & 0 & 0 & 1 \end{bmatrix}$$

$${}^0p_3^0 = \begin{bmatrix} a_4c_{123} + a_3c_{12} + a_2c_1 \\ a_4s_{123} + a_3s_{12} + a_2s_1 \\ 0 \end{bmatrix},$$

$${}^1p_3^1 = \begin{bmatrix} c_2a_4c_3 - s_2a_4s_3 + a_3c_2 \\ s_2a_4\ c_3 + c_2a_4s_3 + a_3s_2 \\ 0 \end{bmatrix}, \quad {}^2p_3^2 = \begin{bmatrix} a_4c_3 \\ a_4s_3 \\ 0 \end{bmatrix}$$

By substituting the above formula in to formula (8), the Jacobian matrix of the thumb is expressed as follows:

$$J = [J_1' \quad J_2' \quad J_3']$$

where the Jacobian of each joint of the thumb is given by

$$J_1' = \begin{bmatrix} -c_1(a_4s_{123} + a_3s_{12} + a_2s_1) \\ -s_1(a_4s_{123} + a_3s_{12} + a_2s_1) \\ a_4c_{123} + a_3c_{12} + a_2c_1 \\ s_1 \\ -c_1 \\ 0 \end{bmatrix}$$

$$J_2' = \begin{bmatrix} -c_1(s_2(c_2a_4c_3 - s_2a_4s_3 + a_3c_2) - c_2(s_2a_4\ c_3 + c_2a_4s_3 + a_3s_2)) \\ -s_1((s_2(c_2a_4c_3 - s_2a_4s_3 + a_3c_2) - c_2(s_2a_4\ c_3 + c_2a_4s_3 + a_3s_2)) \\ c_2(c_2a_4c_3 - s_2a_4s_3 + a_3c_2) + (s_1^2 - c_1^2)s_2(s_2a_4\ c_3 + c_2a_4s_3 + a_3s_2) \\ s_1 \\ -c_1 \\ 0 \end{bmatrix}$$

$$J_3' = \begin{bmatrix} -c_1(s_{23}a_4\ c_3 - c_{23}a_4\ s_3) \\ -s_1(s_{23}a_4\ c_3 - c_{23}a_4\ s_3) \\ c_{23}a_4\ c_3 - s_{23}a_4\ c_3 \\ s_1 \\ -c_1 \\ 0 \end{bmatrix}$$

4 TRAJECTORY PLANNING OF THE FINGER

To ensure the steadiness of the fingers and to reduce the impact to the fruits, the trajectory of the fingers is planned by using the S-shaped velocity profile.

4.1 Linear interpolation using parabola transition curve

Cubic polynomial interpolation is adopted to fit the trajectory of the fingers.

$$\theta(t) = a_0 + a_1t + a_2t^2 + a_3t^3 \quad (16)$$

Derivation of θ(t) is done to obtain the function of speed and acceleration with respect to

time. Considering the requirements on motor performance and fruit picking, the gripper is closed for 5s. The rotation angle of the basal joint of the middle finger varies from 0 to 70°, and the initial and final speeds are both 0, thus

$$a_0 = 0,\ a_1 = 0,\quad a_2 = 8.4,\quad a_3 = -1.12 \qquad (17)$$

Matlab is run using the above parameters to obtain the acceleration curve of basal joint of middle finger, as shown in Fig. 7.

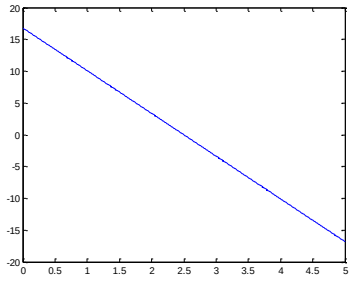

Figure. 7 Acceleration curve of basal joint of middle finger

It can be seen from Fig. 7 that there exists a jump of acceleration at the beginning, causing certain shock to the end effector. Thus the S-shaped speed curve is fitted by parabolic interpolation [20].

For each joint, let t=5s and θ=70 degrees, maximum acceleration a_{max}=20rad/s^2 and maximum speed=20rad/s. At the start, the variable acceleration lasts for 1.5s, constant acceleration for 2s and variable deceleration for 1.5s, followed by constant speed movement for 2s. Substituting these parameters into formula (18), (19) and (20) will result in formula (21). The speed curve and acceleration curve of the basal joint of the middle finger fitted by parabolic interpolation are given in Fig. (8) and (9), respectively.

$$\omega_{1t} = \frac{1}{2}\rho_m t^2 \qquad (18)$$

$$\omega_{2t} = \omega_1 + a_m(t_{a2} - t_{a1}) \qquad (19)$$

$$\omega_{3t} = \theta_2 + (t_{a3} - t_{a2})a_m - \frac{1}{2}\rho_m(t_{a3} - t_{a2})^2 \qquad (20)$$

$$\begin{cases} \omega = 20t^2 & 0 < t < 0.5 \\ \omega = 5 + 20(t-0.5) & 0.5 < t < 1 \\ \omega = 15 + 20(t-1) - 20(t-1)^2 & 1 < t < 1.5 \\ \omega = 20 & 1.5 < t < 3.5 \\ \omega = 15 + 20(-t+4) - 20(-t+4)^2 & 3.5 < t < 4 \\ \omega = 5 - 20(t-4.5) & 4 < t < 4.5 \\ \omega = 20(t-5)^2 & 4.5 < t < 5 \end{cases} \qquad (21)$$

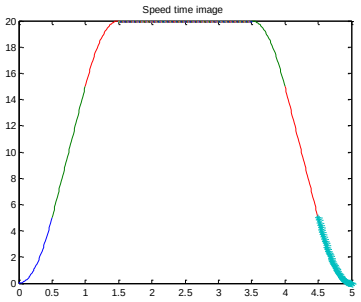

Figure. 8 Speed curve fitted by parabolic interpolation

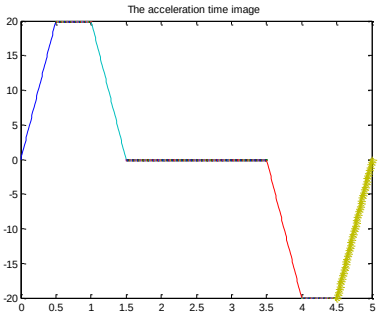

Figure. 9 Acceleration curve fitted by parabolic interpolation

It can be seen from Fig. 8 and Fig. 9 that there is no jump of acceleration and the speed curve is smooth, hence ensuring the steadiness of end effector.

4.2 Kinematic Simulation

The maximum rotation speed of the TRUM-30 type ultrasonic motor is 250r/min. In this case, the gripper is closed for 3s. During this time period, the basal joint of the middle finger rotates by 70 degrees, the middle joint by 22 degrees and the distal interphalangeal joint by 10 degrees. Using these parameters, the stress and motion of the fingers during picking are simulated with SolidWorks software. Kinematic simulation is carried out on the basal joint, middle joint and distal interphalangeal joint of the middle finger. The simulation results are shown in Fig. 10, Fig. 11 and 12.

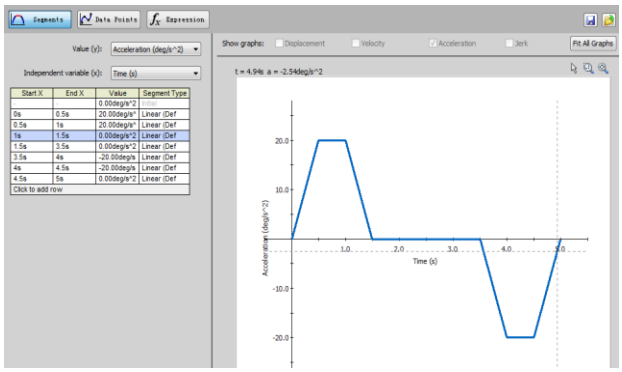

Figure. 10 Kinematic simulation of basal joint of middle finger

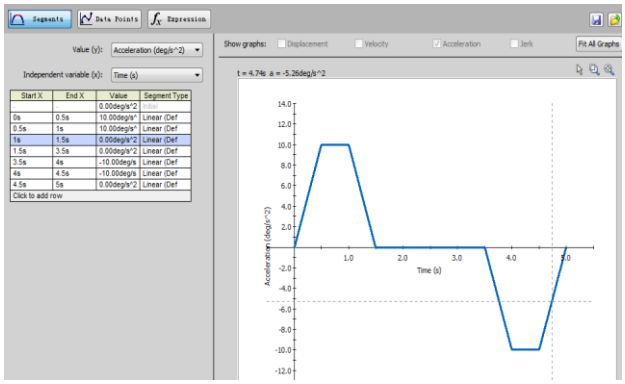

Figure. 11 Kinematic simulation of middle joint of middle finger

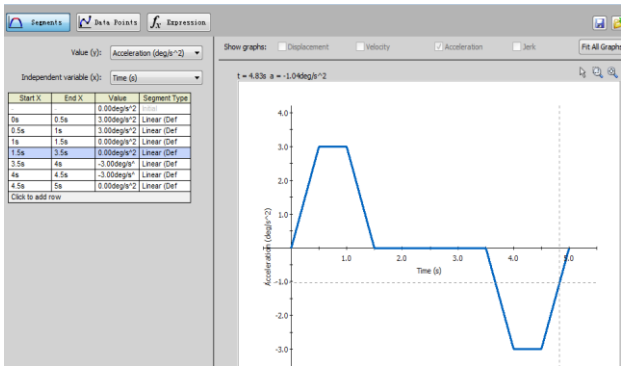

Figure12 Kinematic simulation of distal interphalangeal joint of middle finger

4.3 Calibration of Mechanical Performance of Motor

To achieve high-efficiency fruit picking, the moment of force of the motor has to satisfy relevant performance standards. According to the simulation results in Fig. 10, 11 and 12, the moment of force of the motor is calculated and the motor performance is calibrated.

An apple has a maximum mass of about 0.25kg or 2.45N. That means each finger bears the load of about 0.5N. Since the middle finger bears the largest load in gripping, the stress of the middle finger is calibrated. An external load of 1N is applied perpendicular to each joint of the middle finger. By reference to the results of kinematic simulation in Fig. 10, 11 and 12, the moment of force is obtained for each joint (see Fig. 13, 14 and 15).

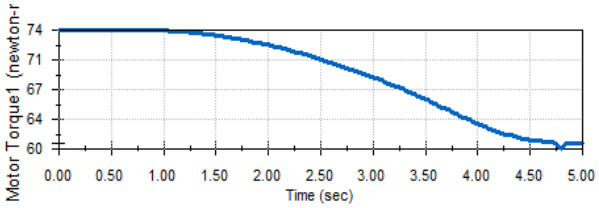

Fig. 13 Moment of force of basal joint of middle finger

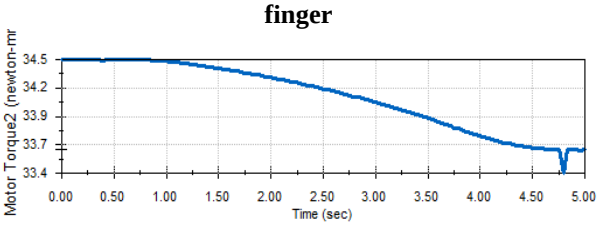

Fig. 14 Moment of force of middle joint of middle finger

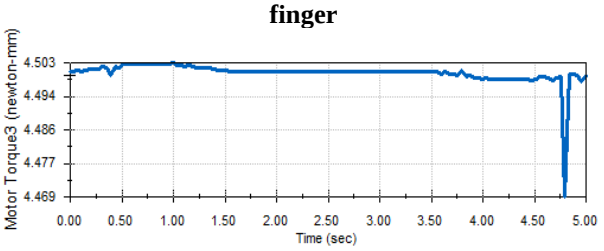

Fig. 15 Moment of force of distal interphalangeal joint of middle finger

It can be seen from the above figure that the maximum moment of force is 74 N•mm for each joint. The maximum torsional moment of TRUM-30 type ultrasonic motor is 200 N•mm, which satisfies the requirement.

5 CONCLUSION

The paper designed an end effector for crawling roundlike fruits such as apples, pears and peaches by mimicking the handling of human hand. This gripper is modularized and had low cost and high interchangeability. To reduce the volume of the end effector, the joints of the fingers were designed as differential mechanisms. The fingers were endowed with degrees of freedom in tilting and lateral swinging. By kinematic analysis and trajectory planning of a single finger, the control of the end effector was realized. Finally, kinematic simulation was carried out using SolidWorks. The paper tested for the motor performance through motion path analysis and confirm that the motion trajectory of the fingers of end effector satisfies the requirement.

6 ACKNOWLEDGEMENTS

This research is supported by science and technology innovation project of Shaanxi Province in China (No. 2015KTZDNY02-05); Students' Innovative Research Plan of Northwest A&F University (No. 2013012545)

7 REFERENCES

►Zhao Yun, Wu Chuangyu, Hu Xudong, Yu Gaohong. Research progress and problems of agricultural robot. Transactions of the Chinese Society of Agricultural Engineering. 2003. 19(1): 20-24 (in Chinese with English abstract).

►Hu Zhiyong, Zhang Xuewei, Zhang Wei, Wang Lin. Precise control of clamping force for watermelon picking end-effector. Transactions of the Chinese Society of Agricultural Engineering. 2014, Vol. 30, No. 17: 43-49.

►Yi-Chich Chiu, Suming Chen, Jia-Feng Lin. Study of an Autonomous Fruit Picking Robot System in Greenhouses. Engineering in Agriculture, Environment and Food. 2013, Vol. 6, No. 3: 92-98.

►Edan Y, Miles G E. Design of an agricultural robot for harvesting melons [J]. Transactions of the ASABE, 1993, 36(2): 593-603.

►Kondo N, ting K C. Robotics for bio-production systems [J]. American Society of Agriculture Engineer, 1998, 62(4): 185-193.

►Reed J N, Miles S J, Butler J. Automatic mushroom Vester development [J]. Journal of Agricultural Engineering Research, 2001, 78: 15-23.

►Zhao De-An, Lv Jidong, Ji Wei, Zhang Ying, Chen Yu. Design and control of an apple harvesting robot. Biosystems Engineering. 2011 Vol. 110, No. 2: 112-122

►Xiangqin Wei a, b, Kun Jia c, Jin hui L and, Yuwei Li c, Yiliang Zeng d, ChunmeiWang a. Automatic method of fruit object extraction under complex agricultural background for vision system of fruit picking robot. Optik. 2014, Vol. 125, No. 19: 5684-5689.

►B. Zion a, M. Mann b, D. Levin a, A. Shilo a; D. Rubinsteinb, I. Shmulevichb. Harvest-order planning for a multiarm robotic harvester. Computers and Electronics in Agriculture. 2014, Vol. 103: 75-81.

►Van Henten, E. J. 1, Van Tuijl, B. A. J. 1, Hemming, J. 1, Kornet, J. G. 1, Bontsema, J. 1, Van Os, E. A. 1. Field Test of an Autonomous Cucumber Picking Robot. Biosystems Engineering. 2003. Vol. 86, No. 3: 305-313.

►M. Monta, N. Kondo, K. C. Ting. End-Effectors for Tomato Harvesting Robot. Artificial Intelligence Review. 1998, Vol. 12, No. 1-3: 11-25.

►Hayashi, Shigehiko 1, Shigematsu, Kenta 1. Evaluation of a strawberry-harvesting robot in a field test. Biosystems Engineering. 2010, Vol. 105, No. 2: 160-171.

►Liu Jizhan, Liu Wei, Mao Hanping, Li Pingping. Analysis on picking plant sequence and route of transplanting robotic for column cultivation. Transactions of the Chinese Society of Agricultural Engineering. 2014, Vol. 30, No. 5: 28-35.

►Cui Peng, Chen Zhi, Zhang Xiao-chao. Statics Analysis of Apple-picking Robot Humanoid manipulator, Transactions of the Chinese Society for Agricultural Machinery. 2011, 42(2): 149-153(in Chinese with English abstract).

►Ji Wei, Li Junle, Yang Jun, et al. Analysis and validation for mechanical damage of apple by gripper in harvesting robot based on finite element method [J]. Transactions of the Chinese Society of Agricultural Engineering, 2015, 31(5): 17-22. (in Chinese with English abstract).

►Grades and specifications of apple [S] NY/T 1793-2009. (in Chinese)

►Fan Shaowei, Liu YiWei, Jin Minghe, Lan Tian, Liu Hong. The anthropomorphic design and experiments of HIT/DLR five-fingered dexterous hand. High Technology Letters. 2009, Vol. 15: No. 3.

►Zhong Liping. Development of Five-fingered Hand Driven by Ultrasonic Motors, Nanjing University of Aeronautics and Astronautics. 2008. 5: 10-11 (in Chinese with English abstract).

►Yu-feng ZHUANG, Dong-qiang LIU, Jun-guang WANG. Dynamic modeling and analyzing of a walking robot. The Journal of China Universities of Posts and Telecommunications. 2014, Vol. 21, No. 1: 122-128.

►Chun Jun Li, ChangLiang Liu, GuChang Wang, Lin Liu, Ye Sun. A Fast Trajectory Planning Algorithm Research for Point-to-Point Motion. Advanced Materials Research. 2014, Vol. 940: 526-530.